UDC 539

Photodisintegration and Virtual State in the Complex Scaling Method

Kato K.[1*], Odsuren M.[2], Kikuchi Y.[3], Myo T.[4], Vasilevsky V.S.[5], Takibayev N.[6]

[1]*Nuclear Reaction Data Centre, Faculty of Science, Hokkaido University, Sapporo 060-0810, Japan*
[2]*School of Engineering and Applied Sciences, National University of Mongolia, Ulaanbaatar 14200, Mongolia* [3]*RIKEN Nishina Center, Wako 351-0198, Japan*
[4]*General Education, Faculty of Engineering, Osaka Institute of Technology, Osaka 535-8585, Japan*
[5]*Bogolyubov Institute for Theoretical Physics, Kiev, Ukraine*
[6]*IETP, Department of Physics and Technology, al-Farabi Kazakh National University, 71 al-Farabi av., 050040 Almaty, Kazakhstan*
[*]*e-mail: kato-iku@gd6.so-net.ne.jp*

The photodisintegration cross section observed just above the neutron threshold energy in ^{9}Be is discussed in the framework of an $\alpha + \alpha + n$ three-cluster model and the complex scaling method. The observed cross sections shows a remarkable sharp peak, which has been discussed in association with photo-neutron reactions in nucleo-syntheses of chemical elements. It is discussed that the enhancement of the peak is understood by taking into account a virtual state but not a resonant state. The complex scaling method cannot reproduce an eigenvalue corresponding to the virtual pole, but provides us with a useful tool for investigation of the photodisintegration cross section.

Key words: photodisintegration cross section, $1/2_1^+$ state of ^{9}Be, virtual state, cluster model, complex scaling method
PACS number(s): 27.20.+n $6 \le A \le 19$, 21.60.Gx, 24.30.Gd, 25.20.Lj

1 Introduction

It is a longstanding problem to determine its resonance energy and width of the first excited $1/2^+$ state of ^{9}Be, which is closely connected with the problem to clarify whether it is a resonant state or not [1 – 7]. Recently, we studied the $1/2^+$ state of ^{9}Be and the photodisintegration cross section (PDXS) applying the complex scaling method (CSM) [8 – 11] to the $\alpha + \alpha + n$ three-cluster model [12, 13]. The results indicate that there is no sharp resonant state corresponding to the distinct peak observed just above the ^{8}Be+n threshold in the photodisintegration cross section of ^{9}Be. On the other hand, the recent experimental cross section data [14 – 16] can be well explained by the $\alpha + \alpha + n$ calculation. From these results, we concluded that the first excited $1/2^+$ state in ^{9}Be is a $^8\mathrm{Be}+n$ virtual state but not resonant one.

The virtual states in nuclear systems have been discussed in the $T = 1$ states of two-nucleon systems for a long time [17, 18], and recently they attract much interest again in association with weak binding problems of neutron rich nuclei [19 – 21]. The low-energy photodisintegration reaction of ^{9}Be has also received much attention from the viewpoint of the astrophysical interest [22, 23]. The photodisintegration cross section has been discussed to be negligibly small in the energy region between thresholds of $\alpha + \alpha + n$ (1.5736 MeV) and $^8\mathrm{Be}+n$ (1.6654 MeV) [14, 15, 16]. The observed cross section above the $^8\mathrm{Be}+n$ shows a prominent peak, although there are some discrepancies among the experimental absolute values. The cross section profile has an asymmetric shape and cannot be explained by a simple resonance formula like the Breit-Wigner form.

In next section, we briefly explain the framework of the $\alpha + \alpha + n$ three-body model and the CSM. In section 3, the results are shown. A conclution is given in section 4.

2 Framework

2.1 α + α + n model

We briefly explain the $\alpha + \alpha + n$ three-body model employed in the present work, whose details are given in Ref. [12]. We here solve the Schrödinger equation for the $\alpha + \alpha + n$ system using the orthogonality condition model [26]. The Schrödinger equation is given as

$$\hat{H}\Psi^{\nu}_{J^{\pi}} = E_{\nu}\Psi^{\nu}_{J^{\pi}}, \qquad (1)$$

where J^π is the total spin and parity of the $\alpha + \alpha + n$ system and v is the index of eigenstates. The energy eigenvalue E_v is measured from the $\alpha + \alpha + n$ threshold of ^{9}Be. The Hamiltonian for the relative motion of the $\alpha + \alpha + n$ three-body system is given as

$$\hat{H} = \sum_{i=1}^{3} t_i - T_{c.m.} + \sum_{i=1}^{2} V_{\alpha n}(\xi_i) + V_{\alpha\alpha} + V_{PF} + V_3, \quad (2)$$

where t_i and $T_{c.m.}$ are kinetic operators for each particle and the center-of-mass of the system, respectively. The interaction between the neutron and the$i$th α particle is given as $V_{\alpha n}(\xi_i)$, where ξ_i is the relative coordinate between them. We here employ the KKNN potential [27] for $V_{\alpha n}$. For the α – α interaction $V_{\alpha\alpha}$ we employ the same potential as used in Ref. [12], which is a folding potential of the effective NN interaction and the Coulomb interaction. The pseudopotential $V_{PF} = \lambda |\Phi_{PF}\rangle\langle\Phi_{PF}|$ is the projection operator to remove the Pauli forbidden states from the relative motions of α – α and α – n [28]. The Pauli forbidden state Φ_{PF} is defined as the harmonic oscillator wave functions by assuming the $(0s)^4$ configuration, whose oscillator length is fixed to reproduce the observed charge radius of the α particle. We here take λ as 10^6 MeV.

In the present calculation, we introduces the $\alpha + \alpha + n$ three-body potential V_3. The explicit form of V_3 is given as

$$V_3 = v_3 \exp(-\mu\rho^2), \quad (3)$$

where ρ is the hyper-radius of the $\alpha + \alpha + n$ system. The hyper-radius is defined as $\rho^2 = 2r^2 + (8/9)R^2$, where r is the distance between two α's and R is that between the neutron and the center-of-mass of the α – α subsystem. To reproduce the ground-state properties, we take the strength v_3 and the width μ as 1.10 MeV and 0.02 fm^{-2}, respectively. For other spin-parity states, we employ the same value of μ as used in $3/2^-$ states, but different strengths are used to reproduce the energy positions of the observed peaks in the photodisintegration cross section.

We solve the Schrödinger equation with the coupled rearrangement-channel Gaussian expansion method [29]. In the present calculation, the ^{9}Be wave function $\Phi^v_{J^\pi}$ is described in the Jacobi coordinate system as

$$\Phi^v_{J^\pi} = \sum_{cij} C^v_{cij}(J^\pi)\left[\left[\phi^i_l(r_c)\phi^j_L(R_c)\right]_I, \chi_{1/2}\right]_{J^\pi}, \quad (4)$$

where $C^v_{cij}(J^\pi)$ is a expansion coefficient and $\chi_{1/2}$ is the spin wave function. The relative coordinates$\mathbf{r}_c$ and $\mathbf{R}_c$ are those in three kinds of the Jacobi coordinate systems indexed by c = (1, 2, 3), and the indices for the basis functions are represented as i and j. The spatial part of the wave function is expanded with the Gaussian basis functions [29].

2.2 Complex scaling method

To calculate the photodisintegration cross section, we use the complex scaling method (CSM) [24, 25]. In the CSM, the relative coordinates ξ ($\mathbf{r}_c$ and $\mathbf{R}_c$) are transformed as

$$U(\theta)\xi U^{-1}(\theta) = \xi e^{i\theta}, \quad (5)$$

where $U(\theta)$ is a complex scaling operator and θ is a scaling angle being a real number. Applying this transformation to Eq. (1), we obtain the complex-scaled Schrödinger equation as

$$\hat{H}^\theta \Psi^v_{J^\pi}(\theta) = E^\theta_v \Psi^v_{J^\pi}(\theta). \quad (6)$$

By solving the complex-scaled Schrödinger equation with appropriate L^2 basis functions, we obtain the energy eigenvalues E^θ_v and eigenstates $\Psi^v_{J^\pi}(\theta)$ (their biorthogonal states $\tilde{\Psi}^v_{J^\pi}(\theta)$) [24, 25].

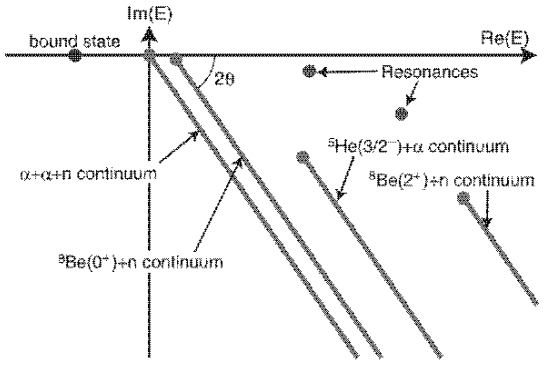

Figure 1 – Schematic picture of energy eigenvalue distribution on the complex energy plane for the $\alpha + \alpha + n$ system

The energy eigenvalues E_ν^θ obtained on the complex energy plane are governed by the ABC theorem [8, 9]. A schematic picture of the energy eigenvalue distribution is shown in Fig. 1. In the CSM, the energies of bound states are given by real numbers and are invariant under the complex scaling. On the other hand, resonances and continuum states are obtained as eigenstates with complex energy eigenvalues. The resonances are obtained as isolated eigenstates on the complex energy plane, whose energies are given as $E_\nu^\theta = E_\nu^r - i\Gamma_\nu/2$. The resonance energies E_ν^r and the decay widths Γ_ν are independent of the scaling angle θ. The complex-scaled continuum states are obtained on branch cuts rotated down by 2θ as shown in Fig. 1. The branch cuts start from the different thresholds for two- and three-body continuum states in the case of the $\alpha + \alpha + n$ system as shown in Fig. 1. This classification of the continuum states is useful in investigation of properties of the ^{9}Be photodisintegration.

Using the energy eigenvalues and eigenstates of the complex-scaled Hamiltonian $\hat{H}^\theta$, we define the complex-scaled Green's function as

$$G^\theta(E;\xi,\xi') = \left\langle \xi \left| \frac{1}{E-\hat{H}^\theta} \right| \xi' \right\rangle = \sum_\nu \int \frac{\Psi^\nu_{J^\pi}(\theta)\tilde{\Psi}^\nu_{J^\pi}(\theta)}{E-E\theta_\nu}. \quad (7)$$

In the derivation of the right-hand side of Eq. (7), we use the extended completeness relation, whose detailed explanation is given in Ref. [30].

We calculate the cross section of ^{9}Be $(3/2^-) + \gamma \to \alpha + \alpha + n$ in terms of the electromagnetic multipole responses. In the present calculation, we focus on the low-lying region of the photodisintegration cross section and take into account only the dipole responses. The photodisintegration cross section σ^γ is given by the sum of those by the $E1$ and $M1$ transitions as

$$\sigma^\gamma(E_\gamma) = \sigma_{E1}(E_\gamma) + \sigma_{M1}(E_\gamma), \quad (8)$$

where E_γ is the incident photon energy. The energy E in Eq. (7) is related to E_γ as $E = E_\gamma - E_{gs}$, where E_{gs} is the binding energy of the ^{9}Be ground state measured from the $\alpha + \alpha + n$ threshold. The cross sections for the electromagnetic dipole transitions σ_{EM1} are expressed as the following form:

$$\sigma_{EM1}(E_\gamma) = \frac{16\pi^3}{9}\left(\frac{E_\gamma}{\hbar c}\right)\frac{dB(EM1,E_\gamma)}{dE_\gamma}. \quad (9)$$

Using the complex-scaled Green's function given in Eq. (7), the electromagnetic dipole transition strength is given as

$$\frac{dB(EM1,E_\gamma)}{dE_\gamma} = -\frac{1}{\pi}\frac{1}{2J_{gs}+1} Im\left[\sum_\nu \int \langle\tilde{\Psi}_{gs}(\theta)\| \hat{O}^\theta_{EM1} \|\Psi^\nu(\theta)\rangle \times \frac{1}{E-E^\theta_\nu}\langle\tilde{\Psi}^\nu(\theta)\| \hat{O}^\theta_{EM1} \|\Psi_{gs}(\theta)\rangle\right], \quad (10)$$

where J_{gs} and Ψ_{gs} (θ) are the total spin and the wave function of the ground state, respectively, and $\hat{O}^\theta_{EM1}$ is an electromagnetic dipole transition operator.

3 Results

We first show the calculated ground-state properties of ^{9}Be and their v_3 dependence. The calculated binding energy and charge and matter radii are listed in Table 1. Without the three-body potential in Eq. (2), the binding energy of the ^{9}Be ground state is overbound and the charge radius is slightly small compared to experiments. To reproduce these quantities, we need the repulsive three-body potential whose parameters are given as $v_3 = 1.10$ MeV and $\mu = 0.02$ fm^{-2}. As results, we reproduce the binding energy and charge radius of the ^{9}Be ground state simultaneously, while the matter radius is slightly larger than the observed one.

Table 1 – ^{9}Be ground-state properties in comparison with experiments. The calculated binding energies E_{gs} in MeV, charge radii R_{ch}, and matter radii R_m with different three-body potential strengths v_3 are listed.

v_3 (MeV)	E_{gs} (MeV)	R_{ch} (fm)	R_m (fm)
.0	2.14	2.50	2.39
.10	1.57	2.53	2.42
exp.	1.5736[32]	2.519 ± 0.012 [33]	2.38 ± 0.01 [34]

Next we confirm that no resonance of the $1/2^+$ state is found with the three-body potential given in Table 1 for the θ = 15° case. We discuss the photodisintegration cross section to $1/2^+$ states. In the present calculation, we fix the ground-state wave function obtained with the three-body potential in Table 1. In Fig. 2, we show the calculated cross sections using Eq. (9) in comparison with the two sets of the observed data [14, 15] which commonly have peaks just above the ^{8}Be $+n$ threshold. The dashed and dotted lines show the cross sections with and without the three-body potential for excited $1/2^+$ states, respectively, whose parameters are the same as those in Table 1. In both results, the calculated cross sections underestimate the low-lying peak above the ^{8}Be $+n$ threshold.

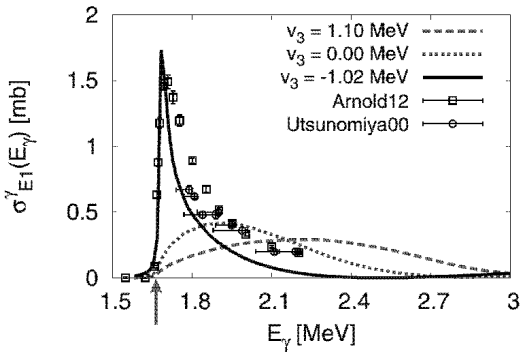

Figure 2 – Calculated photodisintegration cross sections in comparison with experimental data. The arrow indicates the threshold energy of the ^{8}Be(0^+) + n channel

To discuss the observed sharp peak just above the ^{8} Be $+n$ threshold in the photodisintegration cross section, we change the strength v_3 for the $1/2^+$ state to fit the observed data, but its range μ is fixed as the same as used in the ground state. We here take the strength as v_3 = – 1.02 MeV for the $1/2^+$ state and obtain the cross section as shown by the solid line in Fig. 2. Our result reproduces the observed peak by using the attractive three-body potential. The origin of the three-body potential would be a strong state-dependent tensor force and an antisymmetrization of the nucleon among different three clusters. It can be estimated that the tensor force gives a repulsive effect for a p -shell neutron around two α clusters but an attractive one for a higher s-shell neutron [31]. We confirm that the calculated cross section rapidly increases just above the ^{8}Be $+n$ threshold and there is negligibly small strength below this threshold. We also find that the calculated cross sections show the strong dependence on the strengths of the three-body potentials as shown in Fig. 2. This result is interesting and suggests the existence of the three-body unbound state of ^{9}Be$(1/2^+)$, such as a resonance or virtual state. In relation to the cross section, we discuss the character of the $1/2^+$ state.

To see the origin of the low-lying peak above the ^{8}Be $+n$ threshold in more detail, we show the distribution of the energy eigenvalues of the $1/2^+$ states by using the CSM. In the CSM, continuum states are obtained along the branch cuts which start from the threshold energies and are rotated down by 2θ. A resonance is obtained as a solution with a complex energy of $E_\nu^r - i\Gamma_\nu / 2$ which is isolated from the continuum states. However, the virtual states and broad resonances, which are located on the second Riemann sheet covered by the rotated first Riemann sheet, cannot be obtained as the isolated pole in the CSM. The contributions from these states to the cross section are scattered into the continuum states located on the 2θ lines. In Fig. 3, we show the distribution of the energy eigenvalues for the $1/2^+$ states calculated with v_3 = – 1.02 MeV, which reproduces the observed peak as shown in Fig. 2. In the present calculation, we find no resonances in the energy eigenvalue distribution. All energy eigenvalues are located on the 2θ lines, corresponding to the branch cuts for the $\alpha + \alpha + n$, ^{8}Be $(0^+) + n$, and ^{5}He$(3/2^-)$+α continuum states.

We investigate the contributions of two- and three-body continuum states to the cross section to understand the mechanism of the photodisintegration.

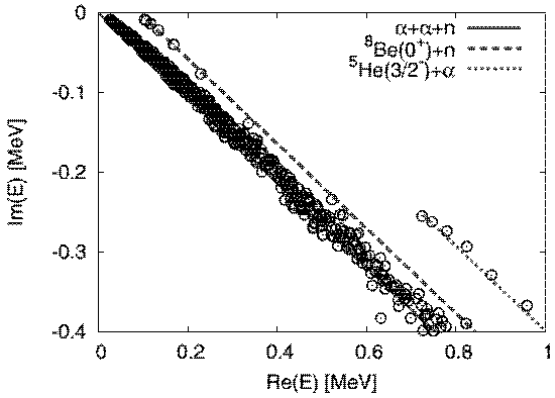

Figure 3 – Distribution of energy eigenvalues of $1/2^+$ states solved with the strength $v_3 = -1.02$ MeV and the scaling angle $\theta = 15^\circ$

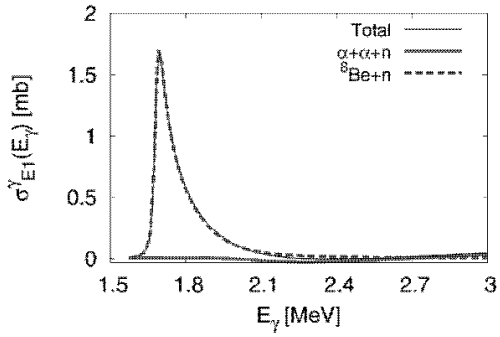

Figure 4 – Decomposed photodisintegration cross sections. The solid and dashed lines are contributions of the $\alpha + \alpha + n$ and ^{8}Be+n continuum states. The black thin line is the same as that in Figure 3

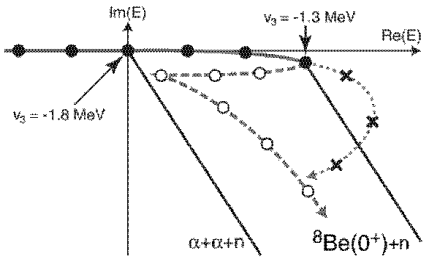

Figure 5 – Pole trajectory of the ^{9}Be $1/2^+$ state in a complex energy plane by changing the three-body potential. The closed circles represent the poles obtained as isolated three-body resonances in CSM. The open circles and crosses are speculated pole positions for the virtual states and broad resonances, respectively

We decompose the cross section calculated with $v_3 = -1.02$ MeV into ^{8}Be$+n$ and $\alpha + \alpha$ components as shown in Fig. 4, to see the dominant contribution in the cross section. The ^{5}He$+\alpha$ contribution is found to be negligible in the low-lying region, and we do not show it in Fig. 4. From Fig. 4, we see that the ^{8}Be$+n$ component is almost identical to the total cross section. This fact indicates that the ^{8}Be+n breakup is dominant in the photodisintegration. This breakup process should be related to the structure of the $1/2^+$ state of ^{9}Be. To investigate the structure of the $1/2^+$ state of ^{9}Be, we calculate the energy eigenvalues of the $\alpha + \alpha + n$ system by changing the strength of the three-body potential v_3, which is shown in Fig. 5. In the present calculation, when the strength of the three-body potential $v_3 = -1.3$ MeV, the resonance pole suddenly appears just below the ^{8}Be$(0^+) + n$ threshold. This resonance pole with a narrow decay width moves smoothly to the bound state region as the three-body potential becomes more attractive, and we finally obtain the ^{9}Be bound state with the region of $v_3 < -1.8$ MeV. On the other hand, we consider the pole trajectory in the opposite case of the three-body potential with $v_3 = -1.3$ MeV. If the resonance exists, the pole with a narrow decay width should appear above the ^{8}Be$+n$ threshold as the analytical continuation from the resonance pole as shown with the crosses in Fig. 5. However, we found that no resonances appear above the ^{8}Be$(0^+) + n$ threshold for $v_3 = -1.3$ MeV of the three-body potential. These facts in the pole trajectory show the possibility of the virtual state of the $1/2^+$ state consisting of ^{8}Be$(0^+) + n$ when we take $v_3 = -1.02$ MeV, which reproduces the experimental cross section. The existence of the virtual state is consistent with the dominant decay into ^{8}Be + n in the photodisintegration of ^{9}Be.

4 Conclusion

We investigate the character of the $1/2^+$ state of ^{9}Be using the photodisintegration reaction with the $\alpha + \alpha + n$ three body model and the CSM. The calculated photodisintegration cross sections into the $1/2^+$ states are shown to have a strong dependence on the strength of the three-body potential for the $1/2^+$ state. The experimental cross section shows a sharp peak just above the ^{8}Be$+n$ threshold, which is nicely reproduced with the attractive three-body potential. We cannot find any resonance poles for the $1/2^+$ states in explaining the peak in the cross section. From the decomposition of the calculated cross section, it is shown that the ^{8}Be $+n$ continuum states dominate the cross section to the $1/2^+$ states. These results indicate the possibility of the virtual-state nature of the first excited $1/2^+$ state. In addition, the pole trajectory suggests that the pole of the $1/2^+$ state is located on the second Riemann sheet of ^{8}Be$+n$ instead of the broad resonances of $\alpha + \alpha + n$.

Acknowledgements

This work was supported by JSPS KAKENHI Grants No. 25400241 and No. 15K05091. The authors are also thankful for the support of the International Collaboration with Al-Farabi Kazakh National University (Grants No. 3106/GF4 and No. 1550/GF3).

References

[1] F. C. Barker. Consistent Description of Unbound States Observed in Scattering and Reactions // Aust. J. Phys. – 1988. – Vol. 41. – P. 743-764.

[2] F. C. Barker. The Low-energy 9Be(γ, n) 8Be Cross Section // Aust. J. Phys. – 2000. – Vol. 53. – P.247-257.

[3] V. Efros and J. Bang. The first excited states of 9Be and 9B // Eur. Phys. J. A. – 1999. – Vol. 4. – P. 33-39.

[4] V. D. Efros, P. von Neumann-Cosel, and A.Richter. Properties of the first excited state of 9Be derived from (γ,n) and (e,e′) reactions // Phys. Rev. C. – 2014. – Vol. 89. – P. 027301.

[5] K. Arai, P. Descouvemont, D. Baye, and W. N. Catford. Resonance structure of 9Be and 9B in a microscopic cluster model // Phys. Rev. C. – 2003. – Vol.68. – P. 014310.

[6] E. Garrido, D. Fedorov, and A. Jensen. Above threshold s-wave resonances illustrated by the 1/2+ states in 9Be and 9B // Phys. Lett. B. – 2010. – Vol. 684. – P.132-136.

[7] R.Álvarez-Rodr uez, A.S. Jensen, E. Garrido, and D. V. Fedorov. Structure and three-body decay of 9Be resonances // Phys. Rev. C. – 2010. – Vol. 82. – P. 034001.

[8] J. Aguilar and J. M. Combes. A class of analytic perturbations for one-body Schrödinger Hamiltonians // Commun. Math. Phys. – 1971 – Vol. 22. – P. 269-279.

[9] E. Balslev and J. M. Combes. Spectral properties of many-body Schrödinger operators with dilatation-analytic interactions // Commun. Math. Phys. – 1971. – Vol. 22. – P. 280-294.

[10] Y. K. Ho. The method of complex coordinate rotation and its applications to atomic collision processes // Phys. Rep. – 1983. – Vol. 99. – P. 1-68.

[11] N. Moiseyev. Quantum theory of resonances: calculating energies, widths and cross-sections by complex scaling // Phys. Rep. – 1998. – Vol. 302. – P.211-293.

[12] M. Odsuren, Y. Kikuchi, T. Myo, M. Aikawa, and K. Kat . Virtual-state character of the 9Be 1/2+ state in the 9Be(γ,n) 8Be reaction // Phys. Rev. C. – 2015. – Vol.92. – P. 014322.

[13] Y. Kikuchi, M. Odsuren, T. Myo, and K. Kat. Photodisintegration cross section of 9Be up to 16 MeV in the α + α + n three-body model // Phys. Rev. C. – 2016. – Vol. 93. – P. 054605.

[14] C. W. Arnoldet al. Cross-section measurement of 9Be(γ,n)8Be and implications for α+α+n→9Be in the r process // Phys. Rev. C. – 2012. – Vol. 85. – P. 044605.

[15] H. Utsunomiyaet al. Photodisintegration of 9Be through the 1/2+ state and cluster dipole resonance // Phys. Rev. C. – 2015. – Vol. 92. – P.064323.

[16] H. Utsunomiya et al. Photodisintegration of 9Be with laser-induced Compton backscattered γ rays // Phys. Rev. C. – 2000. – Vol. 63. – P. 018801.

[17] H. A. Bethe. Eementary Nuclear Theory. – John Wiley and Sons, Inc.: New York, 1947, – 148 p.

[18] S. T. Ma. Interpretation of the Virtual Level of the Deuteron // Rev. Mod. Phys. – 1953. – Vol. 25. – P.853-860.

[19] I.J. Thompson, M.V. Zhukov. Effects of 10Li virtual states on the structure of 11Li // Phys. Rev. C. – 1994. – Vol. 49. – P. 1904-1907.

[20] F.C. Barker, G.T. Hickey. Ground-state configurations of 10Li and 11Li // J. Phys. G. – 1977. – Vol. 3. – P. L23.

[21] H. Masui, S. Aoyama, T. Myo, K. Kat, and K.Ikedad. Study of virtual states in 5He and 10Li with the Jost function method // Nucl. Phys. A. – 2000. – Vol. 673. – P. 207-218.

[22] S. E. Wooseley, R. D. Hoffman. The alpha-process and the r-process. // Astrophys. J. – 1992. – Vol. 395. – P. 202-239.

[23] T. Sasaqui, K. T. Kajino, G. Mathews, K. Otsuki, and T. Nakamura. Sensitivity of r-Process Nucleosynthesis to Light-Element Nuclear Reactions // Astrophys. J. – 2005. – Vol. 634. – P. 1173-1189.

[24] S. Aoyama, T. Myo, K. Kat , and K. Ikeda. The Complex Scaling Method for Many-Body Resonances and Its Applications to Three-Body Resonances // Prog. Theor. Phys. – 2006. – Vol. 116. – P. 1-35.

[25] T. Myo, Y. Kikuchi, H. Masui, and K. Kat . Recent development of complex scaling method for many-body resonances and continua in light nuclei // Prog. Part. Nucl. Phys. – 2014. – Vol. 79. – P. 1-56.

[26] S. Saito. Interaction between Clusters and Pauli Principle // Prog. Theor. Phys. – 1969. – Vol. 41. – P.705-722.

[27] H. Kanada, T. Kaneko, S. Nagata, and M.Nomoto. Microscopic Study of Nucleon-4He Scattering and Effective Nuclear Potentials // Prog. Theor. Phys. 1979. – Vol. 61. – 1327-1341.

[28] V. I. Kukulin, V. M. Krasnopol'sky, V. T. Voronchev, and P. B. Sazonov. Detailed study of the cluster structure of light nuclei in a three-body model: (II). The spectrum of low-lying states of nuclei with A = 6 // Nucl. Phys. A. – 1986. – Vol. 453. – P. 365-388.

[29] E. Hiyama, Y. Kino, and M. Kamimura. Gaussian expansion method for few-body systems // Prog. Part. Nucl. Phys. – 2003. – Vol. 51. – P. 223-307.

[30] T. Myo and K. Kat. Sum Rule Values with Respect to Unbound States in the Complex Scaling Method // Prog. Theor. Phys. 1997. – Vol. 98. – P.1275-1287.

[31] T. Myo, K. Kat , H. Toki, and K. Ikeda. Roles of tensor and pairing correlations on halo formation in 11Li // Phys.Rev.C. – 2007. – Vol. 76. – P. 024305.

[32] D. Tilleyet al. Energy levels of light nuclei A=8,9,10 // Nucl. Phys. A. – 2004. – Vol. 745. – P.155-362.

[33] W. Nörtershäuseret al. Nuclear Charge Radii of 7,9,10Be and the One-Neutron Halo Nucleus 11Be // Phys. Rev. Lett. – 2009. – Vol. 102. – P. 062503.

[34] I. I. Tanihataet al. Measurement of interaction cross sections using isotope beams of Be and B and isospin dependence of the nuclear radii // Phys. Lett. B. – 1988. – Vol. 206. – P. 592-596